ELSEVIER

Thermochimica Acta 395 (2003) 225–236

thermochimica acta

www.elsevier.com/locate/tca

Influence of Cu, Co and Ni cations incorporated in brucite-type layers on thermal behaviour of hydrotalcites and reducibility of the derived mixed oxide systems

Lucjan Chmielarz[a], Piotr Kuśtrowski[a], Alicja Rafalska-Łasocha[a], Roman Dziembaj[b,*]

[a]*Faculty of Chemistry, Jagiellonian University, Ingardena 3, 30-060 Kraków, Poland*
[b]*Regional Laboratory for Physico-chemical Analyses and Structural Studies, Jagiellonian University, Ingardena 3, 30-060 Kraków, Poland*

Received 20 December 2001; received in revised form 26 March 2002; accepted 27 March 2002

Abstract

Thermal decomposition of M–Mg–Al–CO_3–NO_3 hydrotalcites (where M is Cu^{2+}, Co^{2+} or Ni^{2+}) with intended M/Mg (0.10/0.61) and M/Al (0.10/0.29) ratios prepared under the same conditions was studied using high temperature X-ray diffraction (HT-XRD) and thermogravimetry coupling with mass spectrometry (TGA–DTA–MS). Introduction of transition metals to the brucite-like layers of hydrotalcites changed their thermal behaviour. The decomposition of nitrate or carbonate anions was coupled with oxidation from Ni^{2+} to Ni^{3+} and Co^{2+} to Co^{3+}. Further increase of temperature resulted in reduction of these cations. Reduction from Cu^{2+} to Cu^{+} was also observed above 700 °C. Stabilisation of carbonate anions by Cu^{2+} introduced into hydrotalcite matrix was found at temperatures above 600 °C. The thermal treatment of hydrotalcite precursors resulted in the formation of mixed oxide and spinel phases, which were stable after cooling to ambient temperature with exception of CuO phase that appeared during cooling down due to segregation effects. Reducibility of the hydrotalcites calcined at different temperatures was determined by temperature-programmed reduction (TPR) experiments. Specific surface areas of hydrotalcites calcined at 600 °C ranged from 226 to 196 m^2/g dropping with increase in the calcination temperatures to values ranging between 138 and 49 m^2/g depending on transition metal contents.

Keywords: Hydrotalcite-like compounds; Mixed oxides; Spinels; HT-XRD; TGA–DTA–MS; TPR

1. Introduction

Hydrotalcite-type compounds are layered double hydroxides (LDHs) with general formula $[M^{II}_{1-x}M^{III}_{x}(OH)_2]^{x+}[A^{m-}_{x/m}]\cdot nH_2O$, where x may vary in a broad homogeneity range [1]. The structure of these compounds is constituted by brucite-type octahedral layers, in which a part of M^{II} cations (e.g. Mg^{2+}, Cu^{2+}, Co^{2+}, Ni^{2+}, Mn^{2+}, Zn^{2+}, Fe^{2+}) are substituted by M^{III} ones (e.g. Al^{3+}, Cr^{3+}, Fe^{3+}, Co^{3+}, Mn^{3+}, V^{3+}, Ga^{3+}). The resulting excess of positive charge is compensated by hydrated anions in the interlayer space. The CO_3^{2-} ions are the most common in the hydrotalcite-like clays. A variety of

---

[*] Corresponding author. Tel.: +48-12-6324888x2260; fax: +48-12-6340515.
E-mail address: dziembaj@chemia.uj.edu.pl (R. Dziembaj).

PII: S0040-6031(02)00214-9

LDHs have been synthesized, some containing large inorganic polymeric and organic anions [1–3].

Thermal treatments of LDHs lead to dehydration, followed by dehydroxylation and decomposition of anions localized in the interlayers, resulting in the formation of mixed oxides. The mechanism of thermal decomposition of Mg–Al–CO_3–LDH has been described in several papers [4–6]. It is established that Mg–Al–CO_3 hydrotalcites lose water and CO_2 by a cratering mechanism rather than by exfoliation of the metal oxide layers. Such mechanism of H_2O and CO_2 escape causes an increase in the surface area and an appearance of fine pores in the range of 20–40 Å on heating of Mg–Al–CO_3 hydrotalcites [7]. The aluminium content in hydrotalcites seems not to influence the thermal decomposition [8]. An appearance of MgO (periclase) at above 400 °C was confirmed by in situ high temperature X-ray diffraction (HT-XRD) experiments [9]. Further calcination up to about 1000 °C leads to irreversible formation of the spinel phase ($MgAl_2O_4$), found by XRD after cooling.

The calcined LDHs can be used as catalysts with respect to their basic properties, high surface area and thermal stability. Various transition metal cations introduced into the brucite-like layers of LDHs can be precursors of redox- and Lewis-type centres, showing attractive catalytic activity. The mixed oxide catalysts obtained by the thermal decomposition of hydrotalcites containing copper and cobalt were successfully used in the removal of NO_x and SO_x from flue gases [10–16], coupling of phenylethyne [17] or alkylation of phenol [18]. The Ni–Mg–Al mixed oxides systems are extensively studied as catalysts in the partial oxidation of light paraffins [19,20] and hydrogenation of acetonitrile to ethylamine [21].

The catalytic properties of the mixed oxides originating from the LDHs decomposition are greatly influenced by the thermal treatment procedure used. Many authors have described thermal decomposition of LDHs containing transition metal [11,17,20,22–25], however, there are still several open questions. The aim of this paper is to present the influence of Cu^{2+}, Co^{2+} and Ni^{2+} ions incorporated in the brucite-like layers on the thermal stability of the LDHs and the reducibility of the derived mixed oxide systems. A series of a parent Mg–Al–CO_3 and M^{II}–Mg–Al–CO_3 (where M^{II} is Cu^{2+}, Co^{2+} or Ni^{2+}) hydrotalcites have been prepared, maintaining the same content of transition metal, the ratio of $M^{II}/(M^{II}+M^{III})$ and conditions of the synthesis. The prepared LDHs have been investigated by thermogravimetry coupling with mass spectrometry (TGA–DTA–MS) and HT-XRD methods. Moreover, the reducibility and texture of the samples calcined at different temperatures have been determined by temperature-programmed reduction (TPR) and N_2 adsorption at 77 K.

2. Experimental

2.1. Samples preparation

Hydrotalcites with intended compositions: $Mg_{0.71}Al_{0.29}(OH)_2(CO_3)_{0.145}\cdot nH_2O$, $Cu_{0.10}Mg_{0.61}Al_{0.29}(OH)_2(CO_3)_{0.145}\cdot nH_2O$, $Co_{0.10}Mg_{0.61}Al_{0.29}(OH)_2(CO_3)_{0.145}\cdot nH_2O$ and $Ni_{0.10}Mg_{0.61}Al_{0.29}(OH)_2(CO_3)_{0.145}\cdot nH_2O$ were synthesised by co-precipitation from aqueous solutions of suitable metal nitrates—$Mg(NO_3)_2\cdot 6H_2O$ (Sigma), $Al(NO_3)_3\cdot 9H_2O$ (Fluka), $Cu(NO_3)_2\cdot 3H_2O$ (Merck), $Co(NO_3)_2\cdot 6H_2O$ (POCh) and $Ni(NO_3)_2\cdot 6H_2O$ (Aldrich). The solutions of nitrates and NaOH (used as a pH controlling agent) were simultaneously added to a vessel containing a Na_2CO_3 solution at 60 °C (±2 °C) under vigorous stirring. The amount of Na_2CO_3 gave a slight excess in relation to the molar ratio of $[CO_3^{2-}] = 0.5[Al^{3+}]$. The rate of NaOH dosing was carefully controlled in order to keep the pH at constant level of 10.0 ± 0.2. The slurry obtained was stirred at 60 °C for a further 30 min, filtered, washed with distilled water and dried at 120 °C overnight. The samples for BET surface area and TPR measurements were pre-calcined in air at 600, 700, 800 or 900 °C for 16 h.

2.2. Characterisation of hydrotalcites

Chemical analyses of metals were obtained by X-ray fluorescence measurements using a Oxford 2000 instrument. Anion compositions of the samples were determined on the basis of nitrogen and carbon content measured using an EuroVector EA 3000 elemental analyser.

The TGA–DTA–MS measurements of the samples (ca. 20 mg) were carried out using a Mettler Toledo 851^e operated under a flow of pure argon ($80\ cm^3/min$) in the temperature range of 25–1000 °C at a heating rate of 10 °C/min. The gases evolved during the thermal decomposition process were continuously monitored with a quadrupole mass spectrometer ThermoStar (Balzers) connected on-line to the microbalance.

X-ray powder diffraction patterns were recorded on a PW3710 Philips X'pert instrument using Cu Kα radiation ($\lambda = 1.54178$ Å). Structural evolutions during thermal treatment under helium were followed in situ with a HT-XRD attachment. Calcinations were performed from 25 to 1000 °C by steps of 2 h at measurement temperatures. The presented results were confirmed by quantitative phase analysis performed by the Rietveld method. This method takes into account a whole diffraction pattern (with weak, broad and overlapping reflections affected by texture).

The TPR of the calcined samples was carried out in the temperature range of 80–950 °C in a fix bed continuous flow quartz microreactor (i.d. 4.5 mm; l, 240 mm). The flows of gases were controlled by mass flow controllers (Brooks). The hydrogen consumption was monitored on-line by a thermal conductivity detector (Valco) connected to the reactor out-let by a heated line. Prior to the TPR experiments the samples (50 mg), placed in the reactor centre were out-gassed. The TPR runs were carried out with linear heating rate ($\beta = 10$ °C/min) in a flow of 5.22% of H_2 in Ar (20 cm^3/min).

The BET measurements were performed using a ASAP 2010 (Micromeritics). Prior to N_2 adsorption at 77 K, the calcined samples were equilibrated by outgassing at 350 °C under vacuum for 12 h.

3. Results and discussion

3.1. Elemental analysis

Cationic and anionic compositions of the synthesised samples are collected in Table 1. The atomic ratios of metals show that the samples contain lower amounts of aluminium and higher quantities of transition metals than it was supposed. This fact can be explained by incomplete precipitation of Al^{3+} cations during the synthesis carried out in strong basic conditions at pH = 10. The particularly high content of transition metal in the Ni–Mg–Al hydrotalcite is probably caused by replacement of the part of Al^{3+} by Ni^{3+} cations, which could be formed at the high pH level.

Positive charge of brucite-like sheets in the prepared hydrotalcites is counterbalanced mainly by carbonate anions. Small amounts of NO_3^- anions present in the interlayer space of the samples raised from the solution of metal nitrates, which were used as substrates for hydrotalcites syntheses. Surprisingly high quantity of NO_3^- anions is observed in Ni-containing hydrotalcite. The correlation between the presence of Ni^{3+} cations and high content of NO_3^- anions cannot be excluded.

3.2. TGA–DTA–MS measurements

The results of the TGA–DTA analysis of hydrotalcites are presented in Fig. 1, while evolution of the gaseous products of their thermal decomposition are as shown in Fig. 2. Mg–Al hydrotalcite decomposes in two stages with a total mass loss amounted to 45% (Fig. 1A). The endothermic processes of removal of interlayer and weakly adsorbed water took place up to 250 °C. The second stage of Mg–Al hydrotalcite decomposition is endothermic and consists of two unresolved DTG minima at 344 and 400 °C. Water vapour formed from dehydroxylation of OH^- intralayer anions is the main product of thermal decom-

Table 1
Elemental composition of the synthesised samples

Sample	Atomic ratio of metals[a]			Anion distribution[b] (percentage of mass)		Molar ratio of CO_3^{2-}/NO_3^-
	Mg/Al	M[c]/Al	M[c]/Mg	NO_3^-	CO_3^{2-}	
Mg–Al	2.86	–	–	0.50	11.99	24.7
Cu–Mg–Al	2.50	0.58	0.23	0.80	11.41	14.7
Co–Mg–Al	2.53	0.55	0.22	0.52	11.19	22.2
Ni–Mg–Al	2.08	0.72	0.36	4.88	8.75	1.8

[a] Determined by XRF analysis.
[b] Determined by elemental analysis.
[c] M is Cu, Co or Ni.

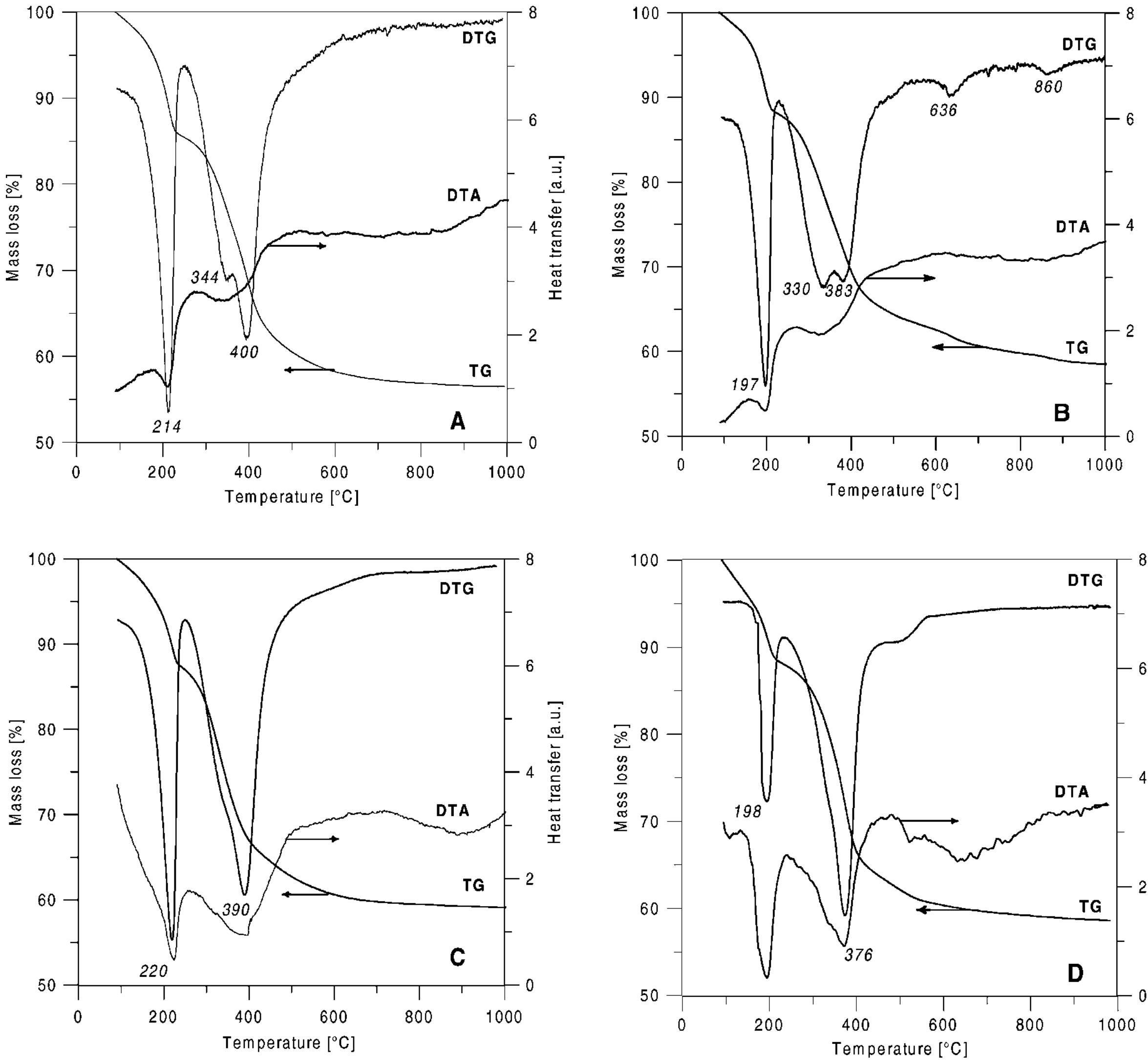

Fig. 1. Results of TGA–DTA analysis of: (A) Mg–Al, (B) Cu–Mg–Al, (C) Co–Mg–Al, and (D) Ni–Mg–Al hydrotalcites.

position of hydrotalcite in this temperature range (Fig. 2A). Moreover, evolution of small amounts of CO_2 and NO, which were formed by thermal decomposition of interlayer anions (CO_3^{2-} and NO_3^{-}), is observed (Fig. 2B and C). It should be noticed that positive charge of brucite-like layers constituted Mg–Al LDH is compensated mainly by carbonates, which decompose at distinctly lower temperature than nitrates (maxima at 430 and 540 °C, respectively).

Partial substitution of Mg cations with Cu, Co or Ni ions resulted in the different thermal decomposition pattern. The total mass loss of transition metal containing hydrotalcites is about 2–3% lower than that obtained for one Mg–Al one.

Removal of interlayer and physisorbed water from Cu–Mg–Al hydrotalcite is manifested by a sharp DTG minimum centred at 197 °C (Fig. 1B). Thermal decomposition of intralayer hydroxyl as well as interlayer carbonate and nitrate anions, which takes place in the temperature range of 250–500 °C, is characterised by two DTG peaks centred at 330 and 383 °C, respectively. It should be stressed that both stages of the Cu–Mg–Al

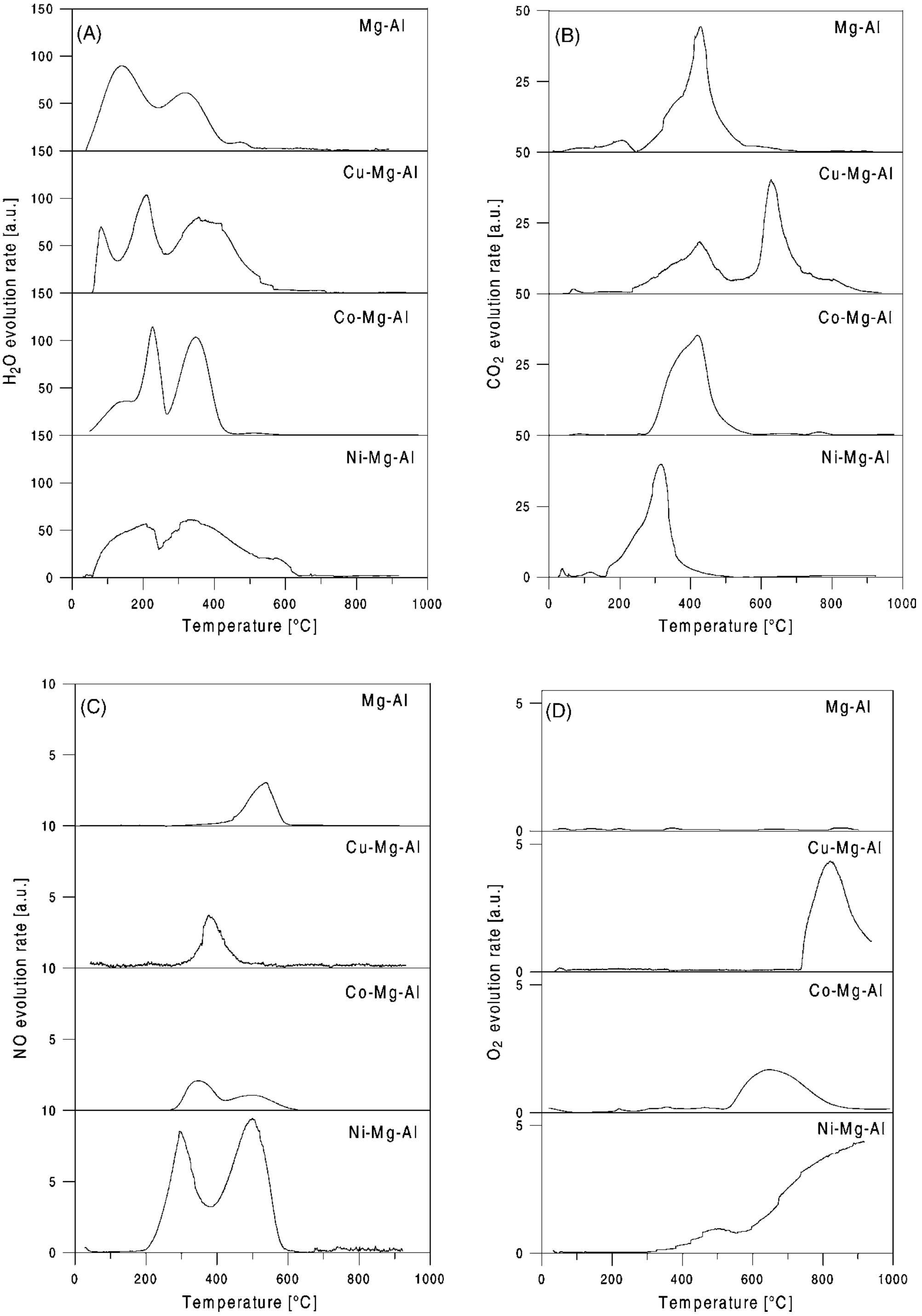

Fig. 2. Evolution of the gaseous products of thermal decompositions of hydrotalcites: (A) H_2O; (B) CO_2; (C) NO; and (D) O_2.

hydrotalcite decomposition occurred at lower temperature than those observed for one Mg–Al one. Positive charge of Cu-containing brucite-like sheets is compensated mainly by carbonates, which are decomposed in two stages with the maxima of CO_2 evolution at 430 and 636 °C, respectively (Fig. 1B and 2B). The high temperature peak of CO_2 emission is characteristic only for the Cu–Mg–Al hydrotalcite, so it seems that copper is responsible for stabilisation of carbonate anions. The Cu-containing sample contained a very small amount of interlayer nitrate anions, which were significantly less stable than those present in the Mg–Al hydrotalcite (Fig. 2C). The DTG peak at about 860 °C (Fig. 1B), as well as the maximum of oxygen evolution (Fig. 2D) observed in the same temperature range can be attributed to the thermal reduction of Cu(II) cations to Cu(I). Such an effect was previously reported for Cu–Mg–Al hydrotalcites derived mixed oxide even in oxygen containing atmosphere [15].

The Co–Mg–Al hydrotalcite loses the interlayer and weakly adsorbed water at temperature below 250 °C (Fig. 1C). The maximum rate of this endothermic process was found at 220 °C. Thermal decomposition of intralayer OH^- and interlayer ${CO_3}^{2-}$ and ${NO_3}^-$ anions is represented by asymmetric DTG peak centred at 390 °C (Fig. 1C). Evolution of carbon dioxide occurs in the temperature range of 260–530 °C (Fig. 2B), whereas, ${NO_3}^-$ anions decomposes in two stages with maxima of NO emission rate at 330 and 490 °C, respectively. At higher temperature the broad peak of oxygen evolution (maximum at about 620 °C) was detected. It seems that thermal treatment of Co–Mg–Al hydrotalcite that occurred in an oxidative atmosphere of evolved gases, formed during the thermal decomposition of interlayer anions (especially NO_x) resulted in partial oxidation of Co^{2+} to Co^{3+} cations. These cations are reduced back at temperature above 700 °C.

The DTG pattern of Ni–Mg–Al hydrotalcite is characterised by a sharp minimum at 198 °C attributed to removal of the interlayer and physisorbed water and by an asymmetric peak at 376 °C with a small shoulder at high temperature side (about 500 °C) connected with thermal decomposition of hydroxyl, carbonate and nitrate anions (Fig. 1D). The evolution of CO_2 occurs at lower temperature than NO, within the range of 170–500 °C (Fig. 2B), while NO is evolved in two distinguished peaks with maxima at 280 and 490 °C (Fig. 2C). Similarly as in the case of Co–Mg–Al hydrotalcite an evolution of oxygen is observed in the high temperature range. However, the process proceeds with slow increase in the intensity when the temperature increase from about 400 to the final of 900 °C.

3.3. XRD study

Fig. 3 presents XRD of the hydrotalcites as well as the products of their thermal decomposition. Obtained results reveal that as-prepared samples have a hexagonal structure with peaks characteristic of hydrotalcites [1]. The comparison of XRD peak's intensities of Ni–Mg–Al, Cu–Mg–Al, Co–Mg–Al and Mg–Al hydrotalcites shows that crystallinity of the first one is lower that those of Cu–Mg–Al, Co–Mg–Al and Mg–Al.

Thermal treatment of the samples has resulted in the changes of their chemical composition and phase content. Heating of well-crystallised hydrotalcites at 220 °C (for Mg–Al and Cu–Mg–Al) or 240 °C (for Co–Mg–Al and Ni–Mg–Al) resulted in the formation of amorphous phases with little remaining of hydrotalcite structure. It should be noticed that both interlayer and weakly adsorbed water were removed from hydrotalcite samples at these temperature (Fig. 1). Thus, loss of the interlayer water destabilised the hydrotalcite structure.

The XRD pattern of Mg–Al sample (Fig. 3A) calcined at 500 °C showed two broad reflections at about 42 and 62° 2θ characteristic of MgO phase. Thermal treatment of the sample at 700 °C resulted in an appearance of a new weak peak at about 34° 2θ which can be attributed to the formation of $MgAl_2O_4$ phase. The increase in calcination temperature to 1000 °C caused increase in crystallinities of MgO and spinel phases.

Introduction of transiton metal into the LDHs influenced strongly the phase composition of the calcined samples. Similar to the Mg–Al sample Cu–Mg–Al one (Fig. 3B) heated in the temperature range of 510–700 °C exhibited maxima characteristic of MgO and spinel phases. Calcination of the Cu–Mg–Al sample at 1000 °C resulted in the increase of crystallinities of these phases. The Rietveld analysis showed that spinel phase consist mainly of $CuAl_2O_4$. We have not found any traces of CuO phase noticed by Kovanda et al. [26] at 800 °C. It should be mentioned, however, that these authors used much higher concentration of Cu in the

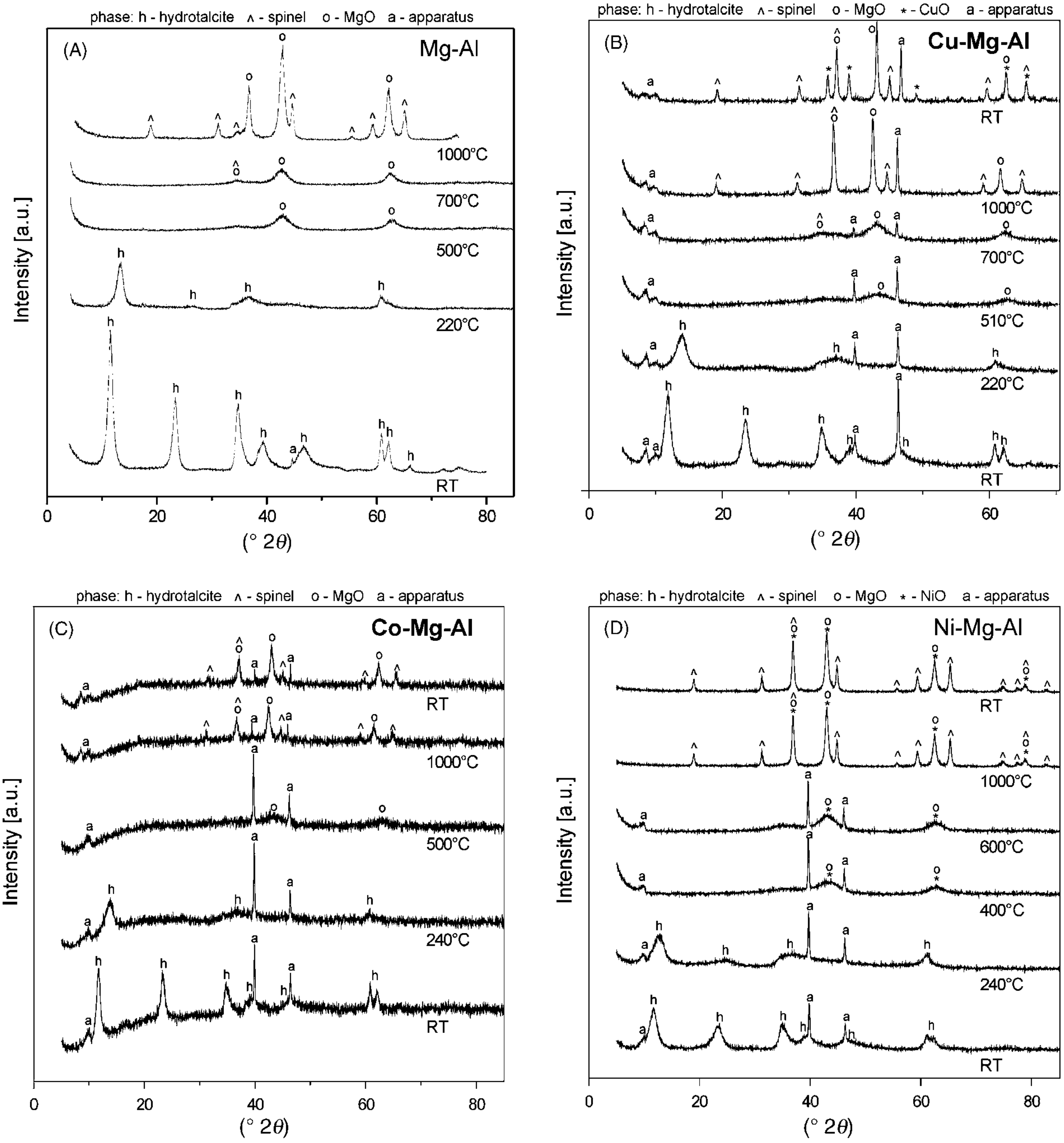

Fig. 3. The HT-XRD patterns of (A) Mg–Al, (B) Cu–Mg–Al, (C) Co–Mg–Al and (D) Ni–Mg–Al samples.

materials. The ratios of Cu/Mg and Cu/Al were equal to 1 in both the cases, while in the presented paper it is only 0.16 and 0.34, respectively. Artizzu et al. [27] noticed traces of CuO phase in the XRD pattern of the sample calcined at 500 °C that showed even lower Cu/Al ratio (0.05), but that sample was obtained by impregnation of previously calcined $MgAl_2O_4$ support at 1000 °C. In our case, the sample was attained by co-

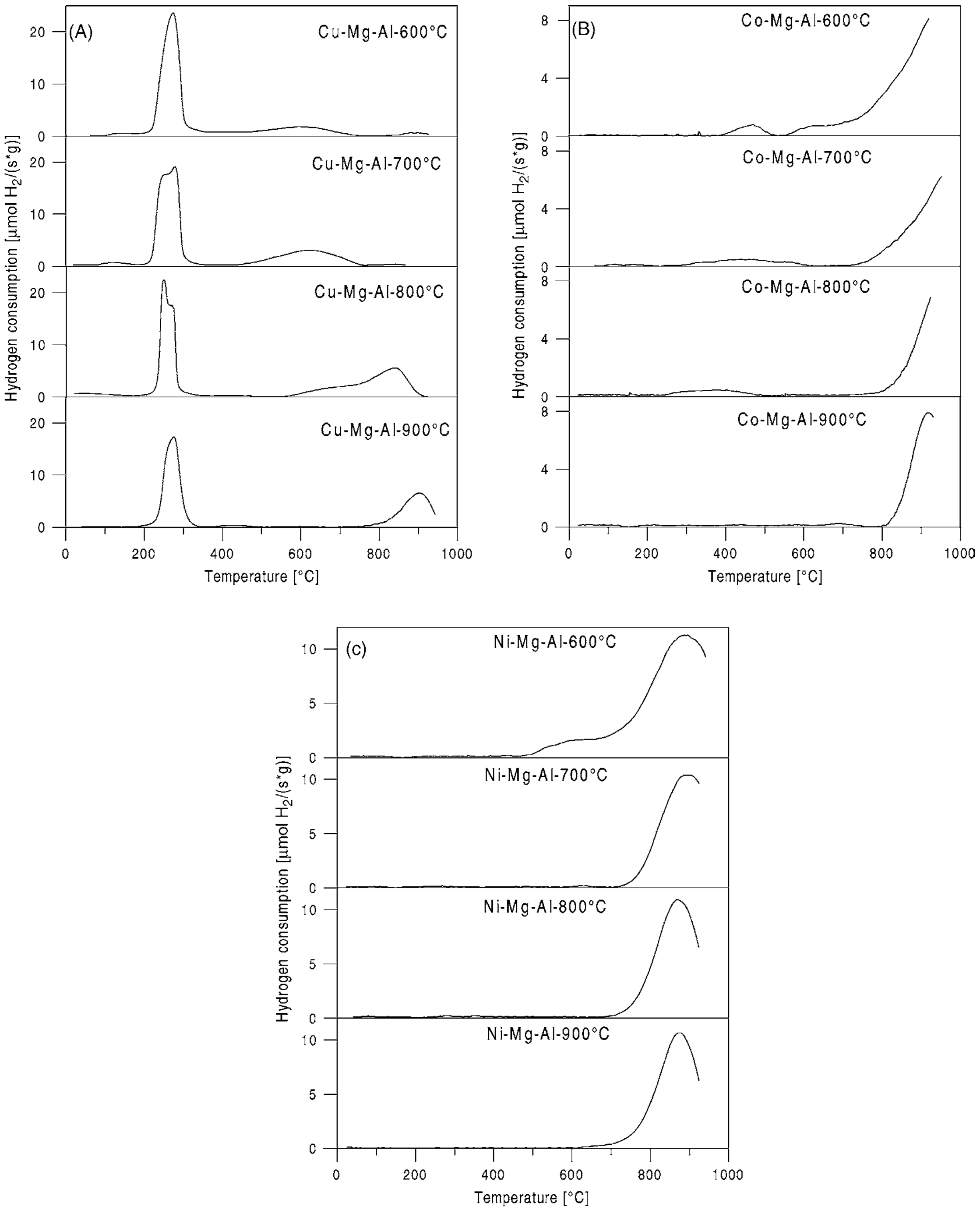

Fig. 4. Results of the TPR of calcined (A) Cu–Mg–Al, (B) Co–Mg–Al and (C) Ni–Mg–Al samples.

precipitation and further calcination of the hydrotalcite phase with incorporated transition metal cations. After heating of our sample up to 1000 °C and then cooling to the room temperature (RT) de-mixing processes were observed and the well crystallized CuO phase appeared in the XRD pattern (Fig. 3B).

Co–Mg–Al hydrotalcite heated at 500 °C was practically amorphous (Fig. 3C). Only very weak and broad reflections (about 43 and 63° 2θ) responsible for the presence of magnesium oxide phase were observed. Increase in the intensities of these peaks and appearance of new ones attributed to well crystallised MgO and spinel phases presence occurred after heating the sample up to 1000 °C. There were practically no changes in XRD pattern after cooling to ambient temperature for the Co–Mg–Al sample.

The decomposition of Ni–Mg–Al sample at 400 °C resulted in the disappearance of XRD reflections attributed to the hydrotalcite phase and formation of very broad and weak peaks related to the presence of a magnesium oxide like phase (Fig. 3D). Increase of temperature to 600 °C caused raise of the intensities of earlier mentioned XRD reflections, while heating of the sample to 1000 °C resulted in appearance of new peaks related to well crystallised $Mg_xNi_{1-x}Al_2O_4$, MgO and NiO phases. The XRD pattern left unchanged after cooling down the sample to the RT.

3.4. Temperature-programmed reduction (TPR)

The reducibility of mixed oxides and spinel systems formed by the thermal decomposition of hydrotalcites at different temperatures was studied by TPR, the spectra are as shown in Fig. 4. The TPR patterns of calcined Cu–Mg–Al sample consist of sharp maxima in the low-temperature range of 200–330 °C and a broad reduction peak above 450 °C (Fig. 4A). The low-temperature peak observed for the sample calcined at 600 °C can be attributed to the reduction of Cu^{2+} cations in CuO. The increase in the calcination temperature results in splitting of low-temperature maximum into two peaks, most probably due to reduction of surface $CuAl_2O_4$ to $CuAlO_2$ [28–30]. At high temperature, reduction of copper in spinel phase takes place. A shift of high temperature TPR peak in the direction of higher temperature is observed for the Cu–Mg–Al sample calcined at 800 or 900 °C, probably due to very slow diffusion of hydrogen in a strongly sintered material. Moreover, the intensity of high-temperature maximum increases because of the higher amount of spinel phase.

The results of the TPR of calcined Co–Mg–Al sample are as shown in Fig. 4B. The TPR pattern of the sample calcined at 600 °C consists of a very small peak at around 480 °C and the main reduction

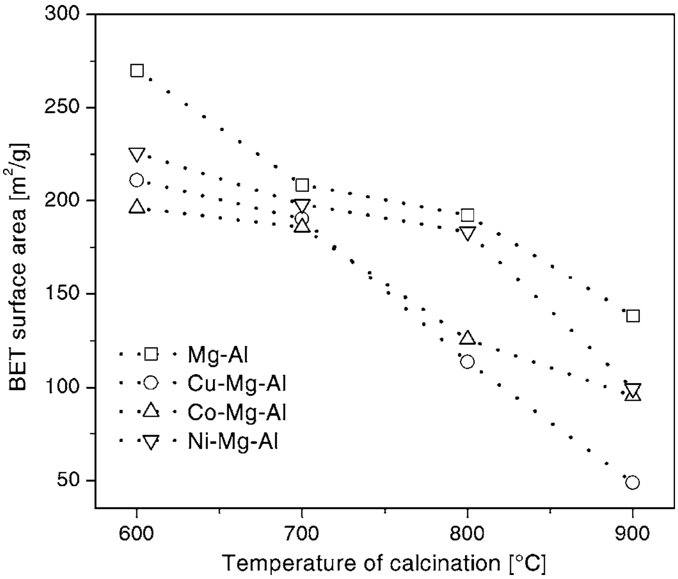

Fig. 5. BET surface areas of hydrotalcite precursors calcined at different temperatures.

stage non-ending up to 950 °C. Taking into account the amount of hydrogen consumed and results of HT-XRD analysis the limited reduction at lower temperature can be attributed to the reduction of small crystallites of segregated Co_3O_4 and surface reduction of Co^{3+}/Co^{2+} cations dissolved in spinel or MgO phases. The main reduction of cobalt cations proceeds above 600 °C as it was notice earlier [31,32]. The last process was so slow that it did not finish at <950 °C.

The TPR patterns of the calcined Ni–Mg–Al hydrotalcite are presented in Fig. 4C. The TPR spectrum of the sample calcined at 600 °C is characterised by at least two unresolved maxima that appeared at temperature above 450 °C. The low-temperature peak must be attributed to the reduction of Ni^{2+} in the NiO phase, while the higher temperature one to the reduction of spinel phase ($NiAl_2O_4$) [19,20,24]. The disappearance of low-temperature maximum in the case of samples calcined at higher temperatures ($T \geq 700$ °C) must be connected with transformation of NiO phase into spinel.

3.5. Textural parameters

The textural properties of Mg–Al, Cu–Mg–Al, Co–Mg–Al and Ni–Mg–Al hydrotalcites calcined at different temperatures (600, 700, 800 and 900 °C) were also investigated. The values of their surface area are presented as shown in Fig. 5. Transition metal containing hydrotalcites were characterised by lower surface areas than the related Mg–Al sample. Introduction of Cu, Co or Ni cations into brucite-like sheets of Mg–Al

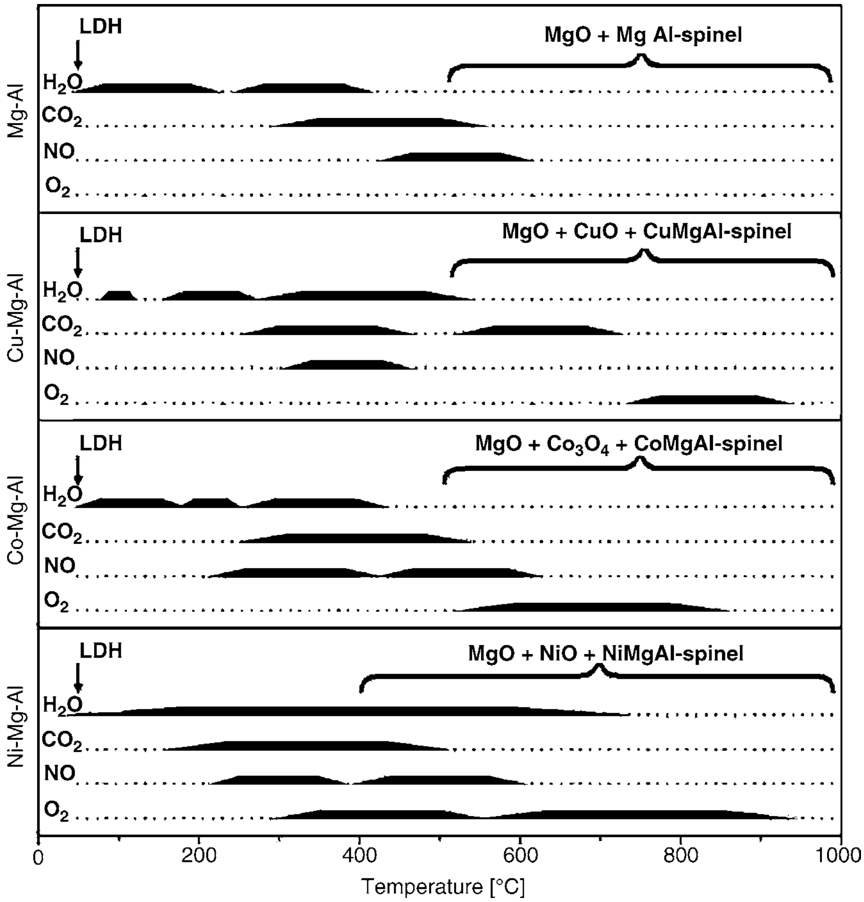

Fig. 6. Comparison of temperature range of phase transformations and the gaseous products evolution obtained from decomposition of various transition metal containing hydrotalcites.

LDH resulted only in small decrease of its surface area observed after calcination at 600 °C from 270 to 196–225 m^2/g. However, it should be noted that the surface area of samples decreased with the increase in the calcination temperature irrespective of metal cations present in LDHs. This effect can be explained by segregation of MgO and spinel as well as sintering of crystallites.

4. Summary

The different transition metal cations (Cu, Co, Ni) incorporated into the brucite-like layers influence strongly thermal decomposition of hydrotalcites and formation of mixed oxide and spinel phases (Fig. 6). The overlapped dehydration and dehydroxylation stages that take place during thermal decomposition of the matrix hydrotalcite phase (Mg–Al) are partially separated. This effect is the most distinct for Cu–Mg–Al hydrotalcite. Copper cations strongly stabilise carbonate anions, while Ni^{2+} shows just opposite effect. The amounts of $NO_3{}^-$ anions intercalated between the brucite-like layer increase about 10 times for Ni-hydrotalcite in comparison to Mg–Al, Cu–Mg–Al and Co–Mg–Al samples. Evolution of oxygen observed for Co–Mg–Al and Ni–Mg–Al hydrotalcites at temperatures above 400 °C is connected with the thermal reduction of Co^{3+} or Ni^{3+}. The M^{3+} cations could be formed by oxidation of M^{2+} cations during the preparation procedure (high value of pH) and/or the thermal treatment in oxidative atmosphere of NO_x/O_2/CO_2 evolved from the decomposition of the interlayer anions. Effect of the thermal reduction of Cu^{2+} is observed at temperatures above 700 °C.

The decomposed LDHs are transferred into amorphous solids at temperatures above 500 °C. At the higher temperatures metal oxides and spinel phases appear. The Rietveld method allowed to determine that the spinel phases consist of mainly transition metal and Al^{3+} cations though a small amount of Mg^{2+} additives cannot be excluded. As regarding Co–Mg–Al and Ni–Mg–Al samples, additionally an appearance of Co_3O_4 and NiO phases observed above 500 °C has been confirmed by the TPR experiments. The XRD reflections characteristic for CuO presence were detected in the calcined Cu–Mg–Al hydrotalcite only after cooling to RT.

The reducibility of the samples depends strongly on the calcination temperature. The great extent of reduction within the low-temperature region (250–350 °C) is observed only for the Cu–Mg–Al system. The splitting of the TPR peaks must be related to reduction of fine crystallites of CuO and surface Cu–Mg–Al spinel phase. The reduction of NiO and $NiAl_2O_4$ as well as Co_3O_4 and Co-aluminates occurs at considerably higher temperatures.

Acknowledgements

Financial support from Polish Committee of Scientific Research (Grant no. PBZ/KBN/018/T09/99/3a) is gratefully acknowledged. The authors would like to thank Ms. Barbara Dudek for her assistance in a running of BET experiments.

References

[1] F. Cavani, F. Trifirò, A. Vaccari, Catal. Today 11 (1991) 173.
[2] S. Miyata, Clays Clay Miner. 23 (1975) 369.
[3] V. Rives, M.A. Ulibarri, Coord. Chem. Rev. 181 (1999) 61.
[4] M.J. Hudson, S. Carlino, D.C. Apperley, J. Mater. Chem. 5 (1995) 323.
[5] T. Hibino, Y. Yamashita, K. Kosuge, A. Tsunashima, Clays Clay Miner. 43 (1995) 427.
[6] M. Bellotto, B. Rebours, O. Clausse, J. Lynch, D. Bazin, E. Elkaim, J. Phys. Chem. 100 (1996) 8535.
[7] W.T. Reichle, S.Y. Kang, D.S. Everhardt, J. Catal. 101 (1986) 352.
[8] F. Rey, V. Fornés, J.M. Rojo, J. Chem. Soc., Faraday Trans. 88 (1992) 2233.
[9] E. Kanezaki, Solid State Ion. 106 (1998) 279.
[10] A. Corma, A.E. Palomares, F. Rey, Appl. Catal. Part B. Environ. 4 (1994) 29.
[11] I.J. Shannon, F. Rey, G. Sankar, J.M. Thomas, T. Maschmeyer, A.M. Waller, A.E. Palomares, A. Corma, A.J. Dent, G.N. Greaves, J. Chem. Soc., Faraday Trans. 92 (1996) 4331.
[12] A.E. Palomares, J.M. López-Nieto, F.J. Lázaro, A. López, A. Corma, Appl. Catal. Part B. Environ. 20 (1999) 257.
[13] S. Kannan, C.S. Swamy, Appl. Catal. Part B. Environ. 3 (1994) 109.
[14] M. Trombetta, G. Ramis, G. Busca, B. Montanari, A. Vaccari, Langmuir 13 (1997) 4628.
[15] B. Montanari, A. Vaccari, M. Gazzano, P. Käßner, H. Papp, W. Makowski, T. Łojewski, R. Dziembaj, Appl. Catal. Part B. Environ. 16 (1996) 205.

[16] L. Chmielarz, P. Kuśtrowski, A. Rafalska-Łasocha, D. Majda, R. Dziembaj, Appl. Catal. Part B. Environ. 35 (2002) 195.
[17] S.M. Auer, R. Wandeler, U. Göbel, A. Baiker, J. Catal. 169 (1997) 1.
[18] S. Velu, C.S. Swamy, Appl. Catal. Part A. Gen. 145 (1996) 141.
[19] F. Basile, L. Basini, M. D'Amore, G. Fornasari, A. Guarinoni, D. Matteuzzi, G. Del Piero, F. Trifirò, A. Vaccari, J. Catal. 173 (1998) 247.
[20] K. Schulze, W. Makowski, R. Chyży, R. Dziembaj, G. Geismar, Appl. Clay Sci. 18 (2001) 59.
[21] B. Coq, D. Tichit, S. Ribet, J. Catal. 189 (2000) 117.
[22] S. Kannan, C.S. Swamy, J. Mater. Sci. 32 (1997) 1623.
[23] F. Medina, R. Dutartre, D. Tichit, B. Coq, N.T. Dung, P. Salagre, J.E. Sueiras, J. Mol. Catal. Part A. Chem. 119 (1997) 201.
[24] O. Lebedeva, D. Tichit, B. Coq, Appl. Catal. Part A. Gen. 183 (1999) 61.
[25] L. Chen, T. Horiuchi, T. Osaki, T. Mori, Appl. Catal. Part B. Environ. 23 (1999) 259.
[26] F. Kovanda, K. Jirátová, J. Rymeš, D. Koloušek, Appl. Clay Sci. 18 (2001) 71.
[27] P. Artizzu, E. Grabowski, M. Primet, Y. Brulle, J. Saint-Just, Catal. Today 47 (1999) 83.
[28] J.A. Anderson, C. Márquez-Alvarez, M.J. López-Muñoz, I. Rodríguez-Ramos, A. Guerrero-Ruiz, Appl. Catal. Part B. Environ. 14 (1997) 189.
[29] W.P. Dow, Y.P. Wang, T.J. Huang, J. Catal. 160 (1996) 155.
[30] M. Frenandez-Garcia, I. Rodríguez-Ramos, P. Ferreira-Aparicio, A. Guerrero-Ruiz, J. Catal. 178 (1998) 253.
[31] R. Oukaci, A.H. Singeton, J.A. Goodwin Jr., Appl. Catal. Part A. Gen. 186 (1999) 129.
[32] A.A. Khassin, T.M. Yurieva, G.N. Kustova, I.S. Itengerg, M.P. Domeshkina, T.A. Krieger, L.M. Plyasova, G.K. Chermashentseva, V.N. Parmon, J. Mol. Catal. 168 (2001) 193.